

Impurity-induced antiferromagnetic phase in a doped Haldane system $\text{Pb}(\text{Ni}_{1-x}\text{Mg}_x)_2\text{V}_2\text{O}_8$

T. Masuda* and K. Uchinokura

Department of Advanced Materials Science, The University of Tokyo, 7-3-1 Hongo, Bunkyo-ku, Tokyo 113-8656, Japan

T. Hayashi and N. Miura

Institute for Solid State Physics, The University of Tokyo, 5-1-5 Kashiwanoha, Kashiwa-shi, Chiba 277-8581, Japan

(Received 14 August 2002; published 8 November 2002)

The impurity-induced antiferromagnetic phase in $\text{Pb}(\text{Ni}_{1-x}\text{Mg}_x)_2\text{V}_2\text{O}_8$ ($x=0.020, 0.010, \text{ and } 0.0050$) is studied by means of heat-capacity and magnetization measurements. One $S=1$ spin is induced by one nonmagnetic impurity, which contributes to the antiferromagnetic phase. The effective interaction between these impurity-induced spins is weak and the number of the spins is a few percent of all spins, which results in the disappearance of the antiferromagnetic phase at an anomalously low magnetic field in the H - T phase diagram.

DOI: 10.1103/PhysRevB.66.174416

PACS number(s): 75.10.Jm, 75.30.Kz, 75.50.Ee

I. INTRODUCTION

Recent interest in quantum-spin systems is focused on spin-gap systems, which are classified into spin-Peierls, spin alternation, dimer, two-leg ladder, and Haldane¹ systems. The ground state of these systems is a nonmagnetic singlet state and, therefore, the spin correlation decays rapidly. In the valence bond solid (VBS) model, which is an approximate model for the one-dimensional $S=1$ (1D) Heisenberg model, it decays exponentially.² A numerical study of the $S=1$ 1D Heisenberg model with open boundary conditions shows that the staggered moment induced at the edge decays exponentially,^{3,4} which is consistent with the VBS model. Experimentally, impurity doping to the spin site is a good probe for the degree of freedom of edge spins. An electron spin resonance (ESR) study on impurity-doped NENP showed the $S=1/2$ states at Ni^{2+} sites around the impurity.^{5,6} To simplify the situation we draw a picture that one nonmagnetic ion induces two $S=1/2$ spins, which is shown in Fig. 1(a).

There are several cases for the impurity-induced spins. If the next-nearest-neighbor interaction is negligible, one nonmagnetic impurity induces two free $S=1/2$ spins which is shown in Fig. 1(a). This was reported in NENP doped with nonmagnetic impurities⁶ and many other Haldane materials. If there is a strong coupling between the edge spins in one separated chain, the configuration of impurity-induced spins is shown in Fig. 1(c). The total spin in a chain with an even number of spins is 0 and the one in a chain with an odd number of spins is 1. In this case two nonmagnetic impurities induce one $S=1$ spin on the average, which was observed only in $\text{Y}_2\text{BaNi}_{1-x}\text{Zn}_x\text{O}_5$.⁷ If the next-nearest-neighbor interaction is ferromagnetic and strong, the adjacent impurity-induced spins will be coupled and form an $S=1$ spin. In this case one nonmagnetic impurity will induce one $S=1$ spin. This case has not been reported experimentally in a real material. In any case most of the spins are in a singlet state and the system would be mapped to the paramagnetic state with a reduced number of spins at low temperatures and at low magnetic fields compared to the spin gap energy.

To observe the degree of freedom of spins or to estimate the number of spins, the heat capacity is one of the best tools. The heat capacity of free spins is expressed by the Schottky heat capacity:

$$C = N \frac{(g \mu_B H)^2}{k_B T^2} \left[\frac{(S+1/2)^2}{\sinh^2[\beta g \mu_B H (S+1/2)]} - \frac{(1/2)^2}{\sinh^2(\beta g \mu_B H)} \right]. \quad (1)$$

The temperature dependences of the Schottky heat capacity are shown in Fig. 2(a) for $S=1/2, 1, \text{ and } 2$. The shapes are quite different among those for different sizes of spins and one can estimate the size of spins, the number of spins, and the g value from the Schottky heat capacity. The magnetic susceptibility also tells us information on the number of spins, the size of spins, and the g value. Figure 2(b) shows the inverse magnetic susceptibility of free spins for four $S=1/2$ spins, two $S=1$ spins, and one $S=2$ spin. In this case,

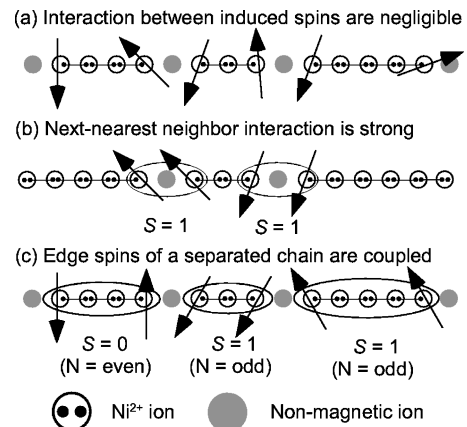


FIG. 1. (a) VBS description when the next-nearest-neighbor interaction is neglected. (b) VBS description when the next-nearest-neighbor interaction is ferromagnetic. (c) Singlet-triplet model.

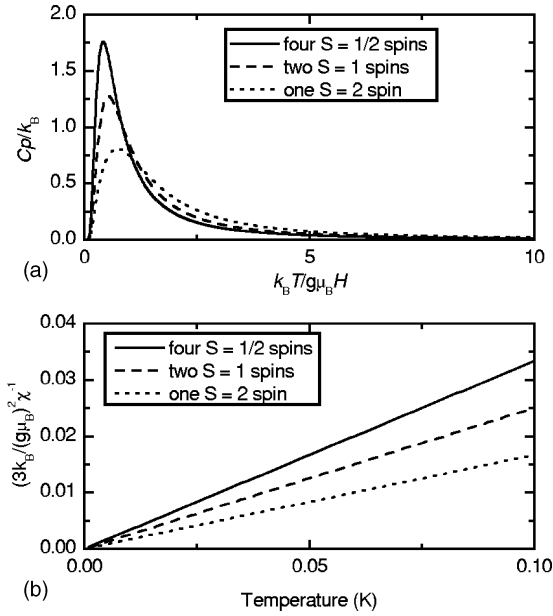


FIG. 2. (a) The Schottky heat capacities for four $S=1/2$ spins, two $S=1$ spins, and one $S=2$ spin. (b) The inverse magnetic susceptibilities for four $S=1/2$ spins, two $S=1$ spins, and one $S=2$ spin.

however, the Curie constant is the product of the number of spins, the size of spins, and the g value and we cannot know each value separately.

In doped Haldane materials the paramagnetic state is strongly fluctuated by quantum effects and the impurity-induced spins are usually not in the ordered state even at low temperatures.^{5–8} If the interchain spin interaction is rather large, however, the impurity-induced spins may be in the ordered state as was observed in a different spin-gap material doped with nonmagnetic impurities $\text{Cu}_{1-x}\text{M}_x\text{GeO}_3$.^{9–12} $\text{Pb}(\text{Ni}_{1-x}\text{Mg}_x)_2\text{V}_2\text{O}_8$ (Ni^{2+} : $S=1$, Mg^{2+} : $S=0$) (Refs. 13 and 14) is an example of the impurity-induced antiferromagnetic (AF) ordered phase in the doped Haldane system because the interchain spin interaction is rather large and $\text{PbNi}_2\text{V}_2\text{O}_8$ is located in the vicinity of the phase boundary between the ordered phase and Haldane phase.¹⁵ The authors of Refs. 13 and 14 observed the AF transition by means of magnetic susceptibility and heat capacity measurements at $T \geq 2$ K in $\text{Pb}(\text{Ni}_{1-x}\text{Mg}_x)_2\text{V}_2\text{O}_8$. However, the Néel temperature of this material is $T \lesssim 3.5$ K and a lower temperature will be required to study the AF phase in more detail. If a small number of spins induced by nonmagnetic ions contribute to the antiferromagnetic order, we can map the original spin system to the antiferromagnetic spin system with a reduced number of spins. In this mapped system the number of (impurity-induced) spins and the (impurity-induced) spin interaction would be small. Therefore, all (impurity-induced) spins would be along the magnetic field and the impurity-induced AF phase would disappear at an anomalously low magnetic field.

In Sec. III we performed the heat capacity measurements down to 0.45 K in $\text{Pb}(\text{Ni}_{1-x}\text{Mg}_x)_2\text{V}_2\text{O}_8$ ($x=0.020$) in the magnetic field and observed the disappearance of the impurity-induced AF phase at 3–4 T. To complete the

magnetic-field–temperature (H - T) phase diagram we performed a magnetization measurement in $\text{Pb}(\text{Ni}_{1-x}\text{Mg}_x)_2\text{V}_2\text{O}_8$ up to 38 T. We confirmed the spin-gap phase at the lowest temperature and the disappearance of the spin gap at high magnetic field. The H - T phase diagram is explained by means of the molecular-field theory very well.

To estimate the degree of freedom of the impurity-induced spins, a heat capacity measurement at lower temperature range would be required. In Sec. IV, therefore, we prepared lower-concentration samples $\text{Pb}(\text{Ni}_{1-x}\text{Mg}_x)_2\text{V}_2\text{O}_8$ ($x=0.005$ and 0.010) which have a lower Néel temperature and performed the heat capacity measurements. Fitting the experimental data to the Schottky heat capacity shows that one nonmagnetic impurity induces one $S=1$ spin. The obtained H - T phase diagrams are explained by the molecular-field theory as well as that in $\text{Pb}(\text{Ni}_{1-x}\text{Mg}_x)_2\text{V}_2\text{O}_8$ ($x=0.020$).

Neutron scattering, of course, will be required for a detailed study of the impurity-induced AF phase but a single crystal of $\text{PbNi}_2\text{V}_2\text{O}_8$ has not been obtained. This material is incongruent and it is difficult to find an adequate condition for the crystal growth. The intensity of the spin-wave excitation in the impurity-induced AF phase is expected to be very small and neutron scattering by means of a polycrystalline sample would not be an effective method to obtain the information on the impurity-induced antiferromagnetic phase.

II. EXPERIMENTAL DETAILS

Polycrystalline samples of $\text{Pb}(\text{Ni}_{1-x}\text{Mg}_x)_2\text{V}_2\text{O}_8$ ($x=0.0050$, 0.010 , and 0.020) were prepared by the solid-state reaction method for heat capacity measurements. For the magnetization measurements, an aligned polycrystalline sample of $\text{Pb}(\text{Ni}_{1-x}\text{Mg}_x)_2\text{V}_2\text{O}_8$ ($x=0.020$) was prepared in the same way as in Ref. 13. Heat capacity measurements were performed down to 0.45 K and up to 14.0 T using a commercial heat capacity measurement system PPMS (Quantum Design Co. Ltd.). The magnetization measurements up to 38 T were performed by means of an induction method using a pair of coaxial pickup coils.

III. $\text{PB}(\text{Ni}_{1-x}\text{MG}_x)_2\text{V}_2\text{O}_8$ ($x=0.020$)

A. Experimental results

The disappearance of the AF phase by a magnetic field is observed in the magnetic heat capacity measurements in $\text{Pb}(\text{Ni}_{1-x}\text{Mg}_x)_2\text{V}_2\text{O}_8$ ($x=0.020$), which is shown in Fig. 3(a). The magnetic heat capacity is obtained by subtracting the heat capacity in $\text{PbMg}_2\text{V}_2\text{O}_8$ from that in $\text{Pb}(\text{Ni}_{1-x}\text{Mg}_x)_2\text{V}_2\text{O}_8$ so as to eliminate approximately the contribution of the lattice heat capacity. The reference compound $\text{PbMg}_2\text{V}_2\text{O}_8$ is isostructural with $\text{PbNi}_2\text{V}_2\text{O}_8$ and the magnetic Ni^{2+} ions are replaced by nonmagnetic ions Mg^{2+} . A sharp peak due to the AF transition is observed at $T=2.2$ K and at 0 T. The peak is suppressed by the magnetic field and it disappears at $H \sim 4$ T. At $H \geq 4$ T broad anomalies are observed and their magnetic field dependence is qualitatively consistent with the Schottky heat capacity assuming that $S=1/2$, g

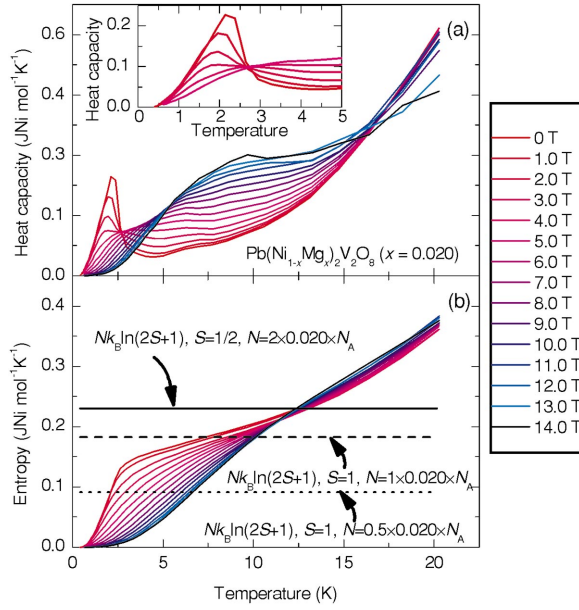


FIG. 3. (a) (Color) Heat capacity in $\text{Pb}(\text{Ni}_{1-x}\text{Mg}_x)_2\text{V}_2\text{O}_8$ ($x = 0.020$). The suppression and disappearance of the AF transition by applying a magnetic field is observed. The broad anomaly at $H \geq 4$ T is the Schottky-like anomaly and it is not due to a phase transition. The inset is the enlargement of the low-temperature and low-magnetic field region. (b) Magnetic entropy estimated from the heat capacity measurements.

$= 2.1$, and the reduced number of free spins, N , is $N = 2 \times 0.020 \times N_A$ [Ni mol^{-1}] or $S = 1$, $g = 2.1$, and $N = 1 \times 0.020 \times N_A$ [Ni mol^{-1}]. Here N_A is the Avogadro number. The Schottky heat capacity, hence, is due to Zeeman splitting of impurity levels. The temperature of the broad anomalies (T_{Schottky}) in the higher magnetic field is $3 \text{ K} \lesssim T_{\text{Schottky}} \lesssim 10 \text{ K}$. The contribution of the spin-gap excitation to heat capacity may not be completely negligible, which results in a difficulty of quantitative consistence.

The magnetic entropy is shown in Fig. 3(b). The solid, dashed, and dotted lines in Fig. 3(b) are the entropies on the assumption of the models described in Figs. 1(a), 1(b), and 1(c), respectively. The magnetic entropy at $H = 0$ T increases drastically at 0.45 K , $\lesssim T \lesssim T_N$, because of the antiferromagnetic order. At $T_N \lesssim T$ the increase of the entropy is due to the AF fluctuation of impurity-induced spins and spin-gap excitation. The spin gap of $\text{PbNi}_2\text{V}_2\text{O}_8$ estimated in Ref. 13 is about 14 K and it is rather difficult to separate the contributions of the AF fluctuation and the spin-gap excitations. However, the magnetic entropy at T_N is well above the dotted line in Fig. 3(b) and the model of either Fig. 1(a) or 1(b) is more adequate than that in Fig. 3(c). We can safely conclude that one nonmagnetic ion induces two $S = 1/2$ spins or one $S = 1$ spin in this system. The degrees of freedom of these spins freeze below T_N , which means that a small number of impurity-induced spins interact with each other weakly and are in an ordered state below T_N . The rest of the spins do not contribute to the entropy or heat capacity at low temperatures, which means that they are in the singlet state and form a spin-gap mode. Hence, spin-gap and antiferromagnetic spin-wave excitations coexist.

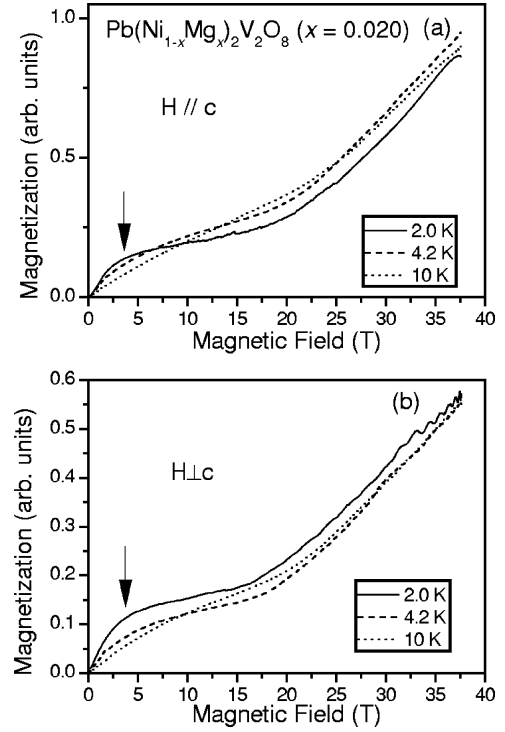


FIG. 4. (a) Magnetization measurements up to 37.5 T in a field parallel to the chain axis. The arrow indicates the magnetic field where the impurity-induced AF phase disappears. (b) Magnetization in a field perpendicular to the chain axis.

The magnetization in $\text{Pb}(\text{Ni}_{1-x}\text{Mg}_x)_2\text{V}_2\text{O}_8$ ($x = 0.020$) in a field parallel [$M_{\parallel}(H)$] and perpendicular [$M_{\perp}(H)$] to the chain axis (the c axis) is shown in Fig. 4. Here the chain axis is also the magnetic easy axis.¹³ The slope of the magnetization curve of 2 K changes at $2\text{--}3 \text{ T}$ in both cases of $H_{\parallel}c$ and $H_{\perp}c$, which is indicated by arrows in Fig. 4. This corresponds to the disappearance of the AF phase which is observed in the heat capacity measurement. At $H \geq 4 \text{ T}$ the impurity-induced spins are along the magnetic field.

At high field an abrupt increase of the magnetization is observed at around 20 T (depending on temperature). Now let us compare this result with the magnetization vs magnetic field (M - H) curve of pure $\text{PbNi}_2\text{V}_2\text{O}_8$ shown in Fig. 2 of Ref. 13. In that figure a sharp change of dM/dH at 4.2 K was observed. This fact was one of the clearest pieces of evidence of the existence of a Haldane gap in pure $\text{PbNi}_2\text{V}_2\text{O}_8$ and the authors of Ref. 13 concluded that $\text{PbNi}_2\text{V}_2\text{O}_8$ is a Haldane-gap system.

The present experiment in $\text{Pb}(\text{Ni}_{1-x}\text{Mg}_x)_2\text{V}_2\text{O}_8$ does not show such a sharp change of dM/dH at the same temperature 4.2 K . However, the magnetic fields of the kinks in both samples are almost the same and the overall behavior (except for the low-field region) is very similar. These facts clearly suggest that both of the kinks in pure $\text{PbNi}_2\text{V}_2\text{O}_8$ and $\text{Pb}(\text{Ni}_{1-x}\text{Mg}_x)_2\text{V}_2\text{O}_8$ originate from the same phenomenon. It leads to the conclusion that even the doped sample has a Haldane-gap-like excitation, at least just below the magnetic field of the kink.

The critical fields parallel to the c axis [$H_c^{\parallel}(2 \text{ K})$] and perpendicular to the c axis [$pH_c^{\perp}(2 \text{ K})$] were 20.8 T and 18.7

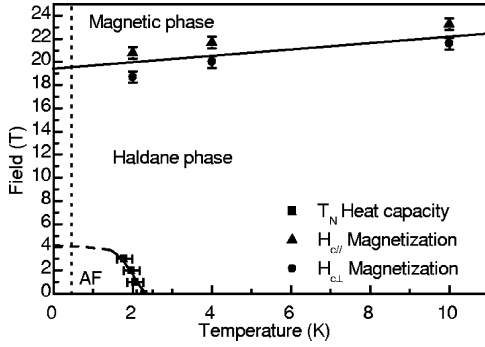


FIG. 5. The magnetic-field-temperature (H - T) phase diagram in $\text{Pb}(\text{Ni}_{1-x}\text{Mg}_x)_2\text{V}_2\text{O}_8$ ($x=0.020$).

T , respectively. Using Eq. (2.13.2) in Ref. 16, which relates the critical fields H_c^{\parallel} and H_c^{\perp} to the doublet and singlet gap energies Δ_{\parallel} and Δ_{\perp} for $\text{Pb}(\text{Ni}_{1-x}\text{Mg}_x)_2\text{V}_2\text{O}_8$ ($x=0.020$), we obtain $\Delta_{\parallel}=1.9$ meV, $\Delta_{\perp}=2.4$ meV, the mean gap energy $\Delta=(2\Delta_{\perp}+\Delta_{\parallel})/3=2.3$ meV, and the anisotropy term $D=-0.23$ meV.¹⁷ Δ is larger than that of pure $\text{PbNi}_2\text{V}_2\text{O}_8$ [$\Delta_{\text{pure}}=1.9$ meV (Ref. 13)], which is due to the finite chain effect.¹⁸ It is observed that H_c decreases with decreasing temperature and, hence, Δ also decreases with decreasing temperature as was observed in pure $\text{PbNi}_2\text{V}_2\text{O}_8$,¹⁹ $\text{SrNi}_2\text{V}_2\text{O}_8$,¹⁵ and other Haldane materials.²⁰

The magnetic-field-temperature (H - T) phase diagram is obtained by heat capacity measurements and magnetization measurements, which is shown in Fig. 5. The suppression and disappearance of the impurity-induced AF phase are observed but this behavior is quite different from that in the conventional AF phase in a quasi-1D AF magnet (half-integer spins). The conventional one is, generally, suppressed by the quantum fluctuation of the spins. The magnetic field suppresses the quantum fluctuation and, therefore, the AF phase in the quasi-1D AF magnet is enhanced by the field.^{21,22} The qualitative behavior of the AF phase in the integer-spin quasi-1D AF material, CsNiCl_3 is the same.²³ $\text{Pb}(\text{Ni}_{1-x}\text{Mg}_x)_2\text{V}_2\text{O}_8$ is, however, quite different.

B. Discussion

The reason for the anomalous behavior of the impurity-induced AF phase is that the staggered spins which contribute to the AF order are strongly fluctuated by quantum effects and that the induced staggered spins decay exponentially.²⁻⁴ Hence, we can map the original system to the simplified model: the system with a reduced number of spins, which is shown in Fig. 1(a) or 1(b). In model (a) the spin is $S=1/2$ and the number of spins is $N=2 \times x \times N_A$ or (b) $S=1$, $N=1 \times x \times N_A$, either of which is adequate for the impurity-induced spin system in $\text{Pb}(\text{Ni}_{1-x}\text{Mg}_x)_2\text{V}_2\text{O}_8$. The interaction between the induced spins is different from the original spin interaction between adjacent spins. We assume here that the effective interaction is isotropic and we adopt a very simple model: the molecular-field approximation. The model Hamiltonian is

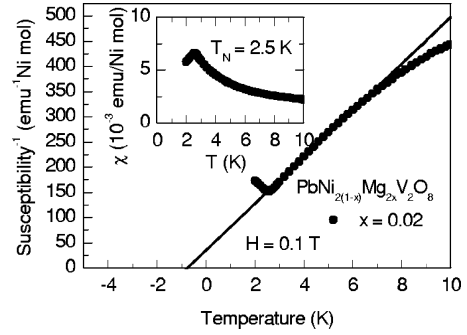


FIG. 6. The inverse magnetic susceptibility in $\text{Pb}(\text{Ni}_{1-x}\text{Mg}_x)_2\text{V}_2\text{O}_8$ ($x=0.020$). The inset is the magnetic susceptibility.

$$H = zJ_{\text{eff}} \sum_{i \in \alpha, j \in \beta} (\langle S \rangle_{\alpha} S_i + \langle S \rangle_{\beta} S_j - \langle S \rangle_{\alpha} \langle S \rangle_{\beta}) - g\mu_B H_z \sum S_i^z. \quad (2)$$

Here z is the coordination number of adjacent spins and J_{eff} is the interaction between the impurity-induced spins. α and β mean the sublattice. There are some relations between molecular-field parameters:

$$\theta = \frac{1}{2} CA, \quad (3)$$

$$A: \text{molecular field constant} \quad A = \frac{2zJ_{\text{eff}}}{Ng^2\mu_B^2}, \quad (4)$$

$$M: \text{saturation moment} \quad M = Ng\mu_B S. \quad (5)$$

Here θ is the Weiss temperature and C is the Curie constant. Using these parameters the saturation field H_0 is

$$H_0 = 2AM. \quad (6)$$

From the heat capacity measurements we assumed that (a) $S=1/2$ and $N=2 \times x \times N_A$ or (b) $S=1$ and $N=1 \times x \times N_A$. We need not make difference between models (a) and (b) when we estimate H_0 in Eq. (6). The molecular field A , which corresponds to the effective interaction, is estimated from the Weiss temperature and the Curie constant. These are obtained by Curie-Weiss fitting in the inverse magnetic susceptibility which is shown in Fig. 6. Half of the molecular-field constant $A/2$ is the y-axis intercept in Fig. 6 and $A=63 \pm 15$ $\text{emu}^{-1}\text{Ni mol}$ is obtained. Hence, $H_0=3.1 \pm 0.8$ T is obtained. This magnetic field is consistent with the value of H , where the impurity-induced AF phase disappears.

IV. $\text{PB}(\text{Ni}_{1-x}\text{MG}_x)_2\text{V}_2\text{O}_8$ ($x=0.0050$ AND 0.010)

A. Experimental results

In the previous section we showed the disappearance of the impurity-induced AF phase at rather low magnetic field. The size of the impurity-induced spins, however, has not been obtained because the temperature and magnetic field ranges are rather high. At higher temperature and magnetic

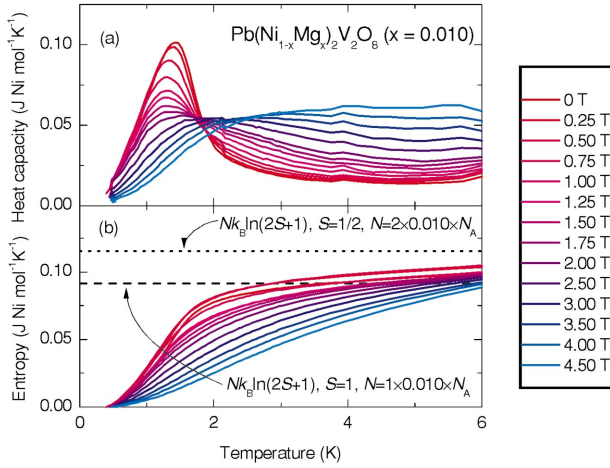


FIG. 7. (Color) The heat capacity in $\text{Pb}(\text{Ni}_{1-x}\text{Mg}_x)_2\text{V}_2\text{O}_8$ ($x = 0.010$).

field the contribution from Haldane-gap excitation cannot be neglected and a quantitative explanation for the Schottky heat capacity was difficult. We therefore performed the heat capacity measurements in the samples $\text{Pb}(\text{Ni}_{1-x}\text{Mg}_x)_2\text{V}_2\text{O}_8$ ($x = 0.010$ and 0.0050), which have lower Néel temperature.

Figures 7(a) and 7(b) show the heat capacity and entropy of the impurity-induced spins, respectively. These data were obtained by subtracting the heat capacity in $\text{PbNi}_2\text{V}_2\text{O}_8$ at $H = 0$ T from that in $\text{Pb}(\text{Ni}_{1-x}\text{Mg}_x)_2\text{V}_2\text{O}_8$ ($x = 0.010$) to eliminate the contribution from phonon and Haldane-gap excitations. The minimum spin gap in $\text{Pb}(\text{Ni}_{1-x}\text{Mg}_x)_2\text{V}_2\text{O}_8$ ($x = 0.020$) in global reciprocal space is estimated as about 20 T in Fig. 5. The temperature and magnetic field are too low for the spin-gap excitation to contribute much to the heat capacity and the subtraction would be valid. An anomaly due to the Néel transition is observed at $T = 1.3$ K and at $H = 0$ T in Fig. 7(a). This anomaly is suppressed with increasing magnetic field and disappears at $H \sim 1.75$ T. The Schottky anomaly, in turn, is observed at $H \gtrsim 1.75$ T. The qualitative behavior is the same as in $\text{Pb}(\text{Ni}_{1-x}\text{Mg}_x)_2\text{V}_2\text{O}_8$ ($x = 0.020$).

The Schottky heat capacity is scaled by the magnetic field as we can see in Eq. (1). We hence show the heat capacity

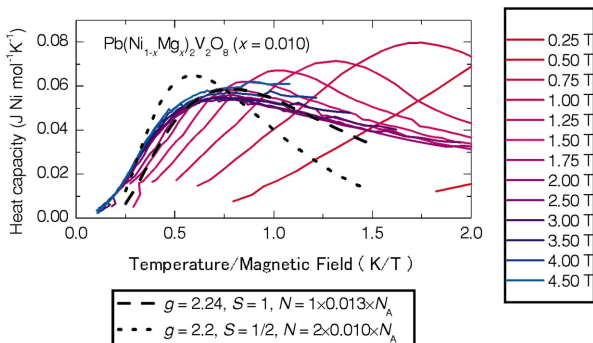


FIG. 8. (Color) The heat capacity in $\text{Pb}(\text{Ni}_{1-x}\text{Mg}_x)_2\text{V}_2\text{O}_8$ ($x = 0.010$) scaled by the magnetic field. The temperature range which is displayed here is $0.40 \text{ K} \leq T \leq 5.0 \text{ K}$ at higher magnetic fields.

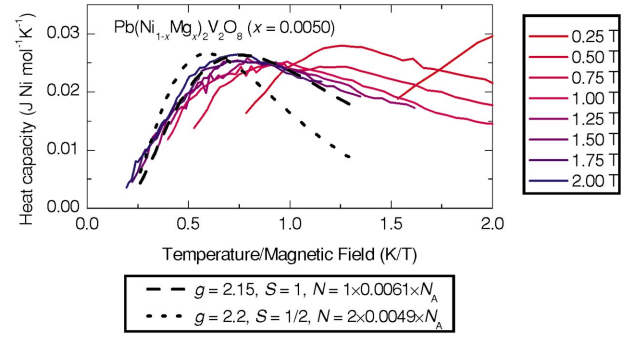


FIG. 9. (Color) The heat capacity in $\text{Pb}(\text{Ni}_{1-x}\text{Mg}_x)_2\text{V}_2\text{O}_8$ ($x = 0.0050$) scaled by the magnetic field. The temperature range which is displayed here is $0.40 \text{ K} \leq T \leq 2.0 \text{ K}$ at higher magnetic fields.

scaled by the magnetic field in Fig. 8. At $H \lesssim 1.75$ T the peak position changes with increasing magnetic field and, on the other hand, at $H \gtrsim 1.75$ T the heat capacities overlap in this scaled temperature. This means that at $H \sim 1.75$ T the applied field is comparable to or larger than the effective field due to the interaction between the impurity-induced spins and the impurity-induced spins are along the magnetic field. At higher magnetic field the interaction between the impurity-induced spins can be negligible and the heat capacity can be fitted by the Schottky heat capacity which is expressed by Eq. (1). The dashed line in Fig. 8 is the best fit when $S = 1$. The fitting parameters are $g = 2.24$ and $N = 1 \times 0.013 \times N_A$. The dotted line is the best fit when $S = 1/2$ and $g = 2.2$. The fitting parameter is $N = 2 \times 0.010 \times N_A$. We obtain a better result when $S = 1/2$, $g = 2.7$, and $N \sim 2 \times 0.01 \times N_A$ than dotted line in Fig. 8 but the g value deviates from 2 very much and we fixed the g value at 2.2. The dashed line is a much better fitting than the dotted line. The imperfection of eliminating the contribution from Haldane-gap excitations may result in a small deviation at higher temperature. Hence, it is concluded that one nonmagnetic ion induces one $S = 1$ spin. The model which is described in Fig. 1(b) is adequate for this material.

The estimated value of $N = 1 \times 0.013 \times N_A$ deviates slightly from $N = 1 \times 0.010 \times N_A$. The impurity concentration is low in this sample and the contribution from the intrinsic vacancies may not be neglected, which would result in the small deviation.

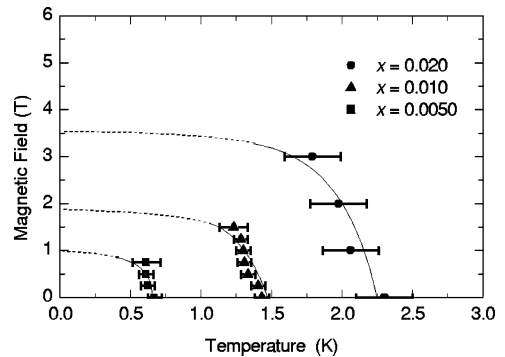


FIG. 10. The H - T phase diagram in $\text{Pb}(\text{Ni}_{1-x}\text{Mg}_x)_2\text{V}_2\text{O}_8$. Solid circles, triangles, and squares show the Néel temperatures in the samples of $x = 0.020$, 0.010 , and 0.0050 .

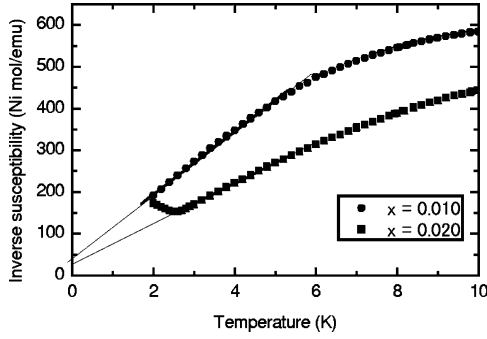


FIG. 11. The inversed magnetic susceptibility in $\text{Pb}(\text{Ni}_{1-x}\text{Mg}_x)_2\text{V}_2\text{O}_8$.

Figure 9 is the heat capacity of the impurity-induced spins in $\text{Pb}(\text{Ni}_{1-x}\text{Mg}_x)_2\text{V}_2\text{O}_8$ ($x=0.0050$) which is obtained in the same way as in $\text{Pb}(\text{Ni}_{1-x}\text{Mg}_x)_2\text{V}_2\text{O}_8$ ($x=0.010$). The temperature is scaled by the magnetic field. The heat capacities overlap with one another at $H \geq 1$ T and they can be fitted by the Schottky heat capacity at this magnetic field region. The obtained parameters are $g=2.15$ and $N=1 \times 0.0061 \times N_A$ when $S=1$ (dashed line). When $S=1/2$, the obtained parameter is $N=2 \times 0.0049 \times N_A$ (dotted line). The dashed line is a much better fitting than the dotted line and the result is consistent with that in $\text{Pb}(\text{Ni}_{1-x}\text{Mg}_x)_2\text{V}_2\text{O}_8$ ($x=0.010$).

The H - T phase diagram at the low magnetic field is shown in Fig. 10. The qualitative behavior is all the same in $\text{Pb}(\text{Ni}_{1-x}\text{Mg}_x)_2\text{V}_2\text{O}_8$. The Néel phases disappear at an anomalously low magnetic field.

B. Discussion

Here we will estimate the critical field H_0 in Eq. (6) for the disappearance of the Néel phase by means of the molecular-field theory as we did in Sec. III. The molecular field constant A in Eq. (4) is estimated to be $A=89 \pm 20 \text{ emu}^{-1} \text{ Ni mol}$ from the magnetic susceptibility measurement which is shown in Fig. 11. By means of Eq. (6), $H_0=2.2 \pm 0.6 \text{ T}$ is obtained in $\text{Pb}(\text{Ni}_{1-x}\text{Mg}_x)_2\text{V}_2\text{O}_8$ ($x=0.010$) and this magnetic field is consistent with the value of H where the impurity-induced AF phase disappears. The same result is obtained in the sample of $x=0.0050$.

We can see that the molecular-field constant A is almost independent of the impurity concentration in Fig. 11. Note that $A/2$ is the y-axis intercept in Fig. 11. Therefore, the critical field H_0 for the disappearance of the Néel phase only depends on the number of impurity-induced spins. The number of spins is the same as that of impurity ions and we can see the approximately proportional relation between the impurity concentration x and the critical field H_0 in Fig. 10.

The disappearance of the “impurity-induced AF phase” at anomalously low magnetic field may be observed in doped CuGeO_3 . The appearance of the AF phase by impurity doping was reported in the two-leg ladder material SrCu_2O_3 (Ref. 24) and dimer material TiCuCl_3 (Ref. 25). If the AF phase of these materials is of the same type as doped $\text{PbNi}_2\text{V}_2\text{O}_8$ or CuGeO_3 , the same phenomenon might be observed. These are future problems.

The fact that one nonmagnetic impurity induces one $S=1$ spin means the existence of a ferromagnetic next-nearest-neighbor (NNN) inchain interaction, which is described in Fig. 1(b). The origin of the NNN interaction is ascribed to the crystal structure of $\text{PbNi}_2\text{V}_2\text{O}_8$. In this material the edge-shared NiO_6 octahedra forms a fourfold screw chain along the b axis.¹³ In this case the nearest-neighbor (NN) and NNN interactions would be comparable and a relatively large NNN interaction is expected. The existence of the NNN interaction (J_{NNN}) is, actually, proposed by Zheleudev *et al.* to explain the spin dispersion in $\text{PbNi}_2\text{V}_2\text{O}_8$.²⁶ Their discussion is qualitatively consistent with our experimental result. Our fits to the data are good if $S=1$ is assumed at $0.40 \text{ K} \leq T \leq 5.0 \text{ K}$ in the sample of $x=0.010$ and at $0.40 \text{ K} \leq T \leq 2.0 \text{ K}$ in the sample of $x=0.0050$. We cannot estimate J_{NNN} from the heat capacity measurements but the success of the fits indicates that J_{NNN} is larger than 5.0 K.

V. SUMMARY

(i) $\text{Pb}(\text{Ni}_{1-x}\text{Mg}_x)_2\text{V}_2\text{O}_8$ ($x=0.020$): we observed that a small number of spins are induced by nonmagnetic ions and they contribute to the impurity-induced AF phase. The disappearance of the AF phase at very low field, 3–4 T, is observed. This is because the number of impurity-induced spins is small and the effective interaction is also small.

(ii) $\text{Pb}(\text{Ni}_{1-x}\text{Mg}_x)_2\text{V}_2\text{O}_8$ ($x=0.010$ and 0.0050): the heat capacity of the impurity-induced spins is explained very well if it is assumed that one nonmagnetic ion induces one spin $S=1$. The existence of a ferromagnetic NNN inchain interaction is suggested. The magnetic field for the disappearance of the AF phase is explained by means of molecular-field theory.

ACKNOWLEDGMENTS

The authors thank I. Tsukada, Y. Uchiyama, and A. Zheleudev for cooperation in the various aspects of this work. This work was supported in part by a Grant-in-Aid for COE Research “Phase Control of Spin-Charge-Photon Coupled System” from the Ministry of Education, Culture, Sports, Science, and Technology.

*Electronic address: tmasuda@k.u-tokyo.ac.jp

¹F. D. M. Haldane, Phys. Rev. Lett. **50**, 1153 (1983).

²I. Affleck, T. Kennedy, E. H. Lieb, and H. Tasaki, Phys. Rev. Lett. **59**, 799 (1987).

³J. Kennedy, J. Phys.: Condens. Matter **2**, 5737 (1990).

⁴S. Miyashita and S. Yamamoto, Phys. Rev. B **48**, 913 (1993).

⁵M. Hagiwara, K. Katsumata, I. Affleck, B. I. Halperin, and J. P. Renard, Phys. Rev. Lett. **65**, 3181 (1990).

⁶S. H. Glarum, S. Geschwind, K. M. Lee, M. L. Kaplan, and J. Michel, Phys. Rev. Lett. **67**, 1614 (1991).

⁷A. P. Ramirez, S-W. Cheong, and M. L. Kaplan, Phys. Rev. Lett. **72**, 3108 (1994).

- ⁸K. Kojima, A. Keren, L. P. Le, G. M. Luke, B. Nachumi, W. D. Wu, Y. J. Uemura, K. Kiyono, S. Miyasaka, H. Takagi, and S. Uchida, *Phys. Rev. Lett.* **74**, 3471 (1995).
- ⁹M. Hase, I. Terasaki, and K. Uchinokura, *Phys. Rev. Lett.* **70**, 3651 (1993).
- ¹⁰M. Hase, I. Terasaki, Y. Sasago, K. Uchinokura, and H. Obara, *Phys. Rev. Lett.* **71**, 4059 (1993).
- ¹¹T. Masuda, A. Fujioka, Y. Uchiyama, I. Tsukada, and K. Uchinokura, *Phys. Rev. Lett.* **80**, 4566 (1998).
- ¹²K. Manabe, H. Ishimoto, N. Koide, Y. Sasago, and K. Uchinokura, *Phys. Rev. B* **58**, R575 (1998).
- ¹³Y. Uchiyama, Y. Sasago, I. Tsukada, K. Uchinokura, A. Zheludev, T. Hayashi, N. Miura, and P. Böni, *Phys. Rev. Lett.* **83**, 632 (1999).
- ¹⁴K. Uchinokura, Y. Uchiyama, T. Masuda, Y. Sasago, I. Tsukada, A. Zheludev, T. Hayashi, N. Miura, and P. Böni, *Physica B* **284-288**, 1641 (2000).
- ¹⁵A. Zheludev, T. Masuda, I. Tsukada, Y. Uchiyama, K. Uchinokura, P. Böni, and S.-H. Lee, *Phys. Rev. B* **62**, 8921 (2000).
- ¹⁶O. Golinelli and Th. Jolicoeur, *J. Phys.: Condens. Matter* **5**, 7847 (1993).
- ¹⁷We should note that these values are not directly related to the intrinsic Haldane gap but to the minimum in the dispersion caused by the interchain interaction. This is the same assumption in Ref. 13. Details are discussed in Ref. 15.
- ¹⁸S. Yamamoto and S. Miyashita, *Phys. Rev. B* **50**, 6277 (1994).
- ¹⁹Y. Uchiyama (unpublished).
- ²⁰A. Zheludev, S. E. Nagler, S. M. Shapiro, L. K. Chou, D. R. Talham, and M. W. Meisel, *Phys. Rev. B* **53**, 15 004 (1996); T. Sakaguchi, K. Kakurai, T. Yokoo, and J. Akimitsu, *J. Phys. Soc. Jpn.* **65**, 3025 (1996).
- ²¹W. J. M. de Jonge, J. P. A. M. Hijmans, F. Boersma, J. C. Schouten, and K. Kopinga, *Phys. Rev. B* **17**, 2922 (1978).
- ²²J. Villain and J. M. Loveluck, *J. Phys. (France) Lett.* **38**, L77 (1977).
- ²³D. Beckmann, J. Wosnitza, H. v. Löhneysen, and D. Visser, *Phys. Rev. Lett.* **71**, 2829 (1993).
- ²⁴M. Azuma, Y. Fujishiro, M. Takano, M. Nohara, and H. Takagi, *Phys. Rev. B* **55**, R8658 (1997).
- ²⁵A. Oosawa, T. Ono, and H. Tanaka, cond-mat/0202004 (unpublished).
- ²⁶A. Zheludev, T. Masuda, K. Uchinokura, and S. E. Nagler, *Phys. Rev. B* **64**, 134415 (2001).